

Amino Acid Adduct Formation by the Nevirapine Metabolite, 12-Hydroxynevirapine—A Possible Factor in Nevirapine Toxicity

Alexandra M. M. Antunes,^{*,†} Ana L. A. Godinho,[†] Inês L. Martins,[†] Gonçalo C. Justino,[†] Frederick A. Beland,[‡] and M. Matilde Marques^{*,†}

Centro de Química Estrutural, Instituto Superior Técnico, Universidade Técnica de Lisboa, 1049-001 Lisboa, Portugal, and Division of Biochemical Toxicology, National Center for Toxicological Research, Jefferson, Arkansas 72079

Received December 14, 2009

Nevirapine (NVP) is a non-nucleoside reverse transcriptase inhibitor used against the human immunodeficiency virus type-1 (HIV-1), mostly to prevent mother-to-child transmission of the virus in developing countries. However, reports of severe NVP-induced hepatotoxicity and serious adverse cutaneous effects have raised concerns about its use. NVP metabolism involves oxidation of the 4-methyl substituent to 4-hydroxymethyl-NVP (12-hydroxy-NVP) and the formation of phenolic derivatives. Further metabolism, through either oxidation to quinoid derivatives or phase II esterification, may produce electrophilic derivatives capable of reacting with bio-nucleophiles to yield covalent adducts. These adducts could potentially be involved in the initiation of toxic responses. To gain insight into potentially reactive sites in proteins and prepare reliable and fully characterized NVP–amino acid adduct standards for subsequent assessment as biomarkers of NVP toxicity, we have used the model electrophile, 12-mesyloxy-NVP, as a synthetic surrogate for the NVP metabolite, 12-sulfoxy-NVP. Reactions of this model ester were conducted with glutathione and the nucleophilic amino acids arginine, cysteine, histidine, and tryptophan. Moreover, because adducts through the N-terminal valine of hemoglobin are convenient biomarkers of exposure to electrophilic toxicants, we also investigated the reaction with valine. We obtained very efficient (>80%) binding through the sulfur of both glutathione and *N*-acetylcysteine and moderate yields (10–14%) for binding through C2 of the indole ring of tryptophan and N1 of the imidazole ring of histidine. Reaction with arginine occurred through the α -amino group, possibly due to the high basicity of the guanidino group in the side chain. Reaction at the α -amino group of valine occurred to a significant extent (33%); the resulting adduct was converted to a thiohydantoin derivative, to obtain a standard useful for prospective biomonitoring studies. All adducts were characterized by a combination of ¹H and ¹³C NMR spectroscopy and mass spectrometry techniques. The NVP conjugates with glutathione and *N*-acetylcysteine identified in this work were previously reported to be formed *in vivo*, although the corresponding structures were not fully characterized. Our results support the validity of 12-mesyloxy-NVP as a surrogate for 12-sulfoxy-NVP and suggest that NVP metabolism to 12-hydroxy-NVP, and subsequent esterification, could potentially be a factor in NVP toxicity. They further imply that multiple sites in proteins may be targets for modification by 12-hydroxy-NVP-derived electrophiles *in vivo*. Additionally, we obtained reliable, fully characterized standards for the assessment of protein modification by NVP *in vivo*, which should help clarify the potential role of metabolism in NVP-induced toxicity.

Introduction

The non-nucleoside reverse transcriptase inhibitor (NNRTI)¹ nevirapine (11-cyclopropyl-5,11-dihydro-4-methyl-6*H*-dipyrido[3,2-*b*:2',3'-*e*][1,4]diazepin-6-one, NVP, **1**; Scheme 1) was the first member of this class approved by the U.S. Food

and Drug Administration for use in combination therapy of human immunodeficiency virus (HIV)-1 infection (*1*). Currently, NVP is still one of the most prescribed antiretroviral drugs, particularly in developing countries, both as a single-dose prophylaxis to prevent mother-to-child HIV transmission and in combination therapy (2–5). Despite its clinical efficacy, NVP administration is associated with a variety of toxic responses, with individual susceptibilities to the adverse effects differing among patients (6–8). As such, the suggestion (9) that extended-dose daily NVP regimens may be adequate to decrease the risk of HIV transmission to breastfed infants in low-resource settings has met criticism, partly on account of toxicity considerations (10). Among the toxicities associated with NVP use, the most severe is hepatotoxicity, which can be fatal in some instances. The most commonly reported side effect is a skin rash, which may be life threatening and eventually leads to discontinuation of the drug.

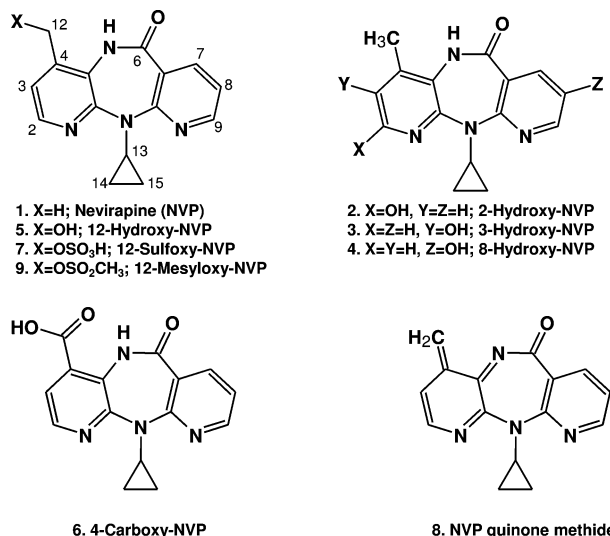
* To whom correspondence should be addressed. (A.M.M.A.) Tel: 351-21-8419388. Fax: 351-21-8464457. E-mail: alexandra.antunes@ist.utl.pt. (M.M.M.) Tel: 351-21-8419200. Fax: 351-21-8464457. E-mail: matilde.marques@ist.utl.pt.

[†] Universidade Técnica de Lisboa.

[‡] National Center for Toxicological Research.

¹ Abbreviations: Boc, *tert*-butoxycarbonyl; *t*-Bu, *tert*-butyl; DMSO, dimethyl sulfoxide; ESI, electrospray ionization; GSH, glutathione; HIV, human immunodeficiency virus; HMBC, heteronuclear multiple bond correlation; HMQC, heteronuclear multiple quantum coherence; HSQC, heteronuclear single quantum coherence; Imid, imidazole; Ind, indole; Me, methyl; MS/MS, tandem mass spectrometry; NNRTI, non-nucleoside reverse transcriptase inhibitor; NOESY, two-dimensional nuclear Overhauser effect spectroscopy; NVP, nevirapine; Ph, phenyl; TOCSY, total correlation spectroscopy; *t*_R, retention time.

Scheme 1. Structures of NVP (1), NVP Metabolites (2–7), and Other NVP Derivatives (8 and 9) Mentioned in the Text



NVP is not mutagenic or clastogenic in a variety of assays, including microbial and mammalian cell gene mutation tests and cytogenetic assays (11). However, in mice administered 0, 50, 375, or 750 mg NVP/kg bw/day, there was an increased incidence of hepatocellular adenomas and carcinomas at all doses in males and at the two highest doses in females (11). Likewise, in rats administered 0, 3.5, 17.5, or 35 mg NVP/kg bw/day, there was an increased incidence of hepatocellular adenomas at all doses in males and at the highest dose in females (11). Although there have been no reports in the literature of any correlation between NVP administration and the development of cancer in humans, the recent suggestion (12) of a possible association between the use of NNRTIs and the occurrence of non-AIDS-defining cancers, predominantly Hodgkin's lymphoma, in HIV-positive individuals warrants further investigation.

The reasons for the adverse effects of NVP administration are currently not clear, although there is increasing evidence that metabolic activation to reactive electrophiles capable of reacting with bionucleophiles is likely to be involved in the initiation of toxic responses. For instance, although the reactive metabolites were not identified, Takakusa et al. (13) reported covalent binding of [¹⁴C]NVP to rat and human liver microsomal proteins in vitro and to liver tissue and plasma proteins from male rats administered 20 mg NVP/kg bw as a single oral dose.

In addition to humans, NVP metabolism has been reported in mice, rats, rabbits, dogs, cynomolgus monkeys, chimpanzees, and baboons (14–18). In all species investigated, phase I metabolism consistently involves oxidation to 2-, 3-, and 8-hydroxy-NVP, 4-hydroxymethyl-NVP (12-hydroxy-NVP, **5**), and 4-carboxy-NVP (**2–6**; Scheme 1). All of the hydroxyl groups are prone to subsequent conjugation to the corresponding glucuronides, which are excreted primarily in the urine. In humans, the formation of 2-hydroxy-NVP is attributed to the P450 3A subfamily, 3-hydroxy-NVP to P450 2B6, 8-hydroxy-NVP to P450 3A4, 2B6, and 2D6, and **5** to P450 3A4 and possibly 2D6 and 2C9 (16).

Although comparatively less information is available about other conjugation pathways, both acetylation and/or sulfonation of the hydroxylated NVP metabolites (e.g., to **7**, Scheme 1) are plausible processes in the liver (19). Likewise, the ring-hydroxylated metabolites may undergo oxidation to *ortho*-quinone or semiquinone species (20). Any of these pathways

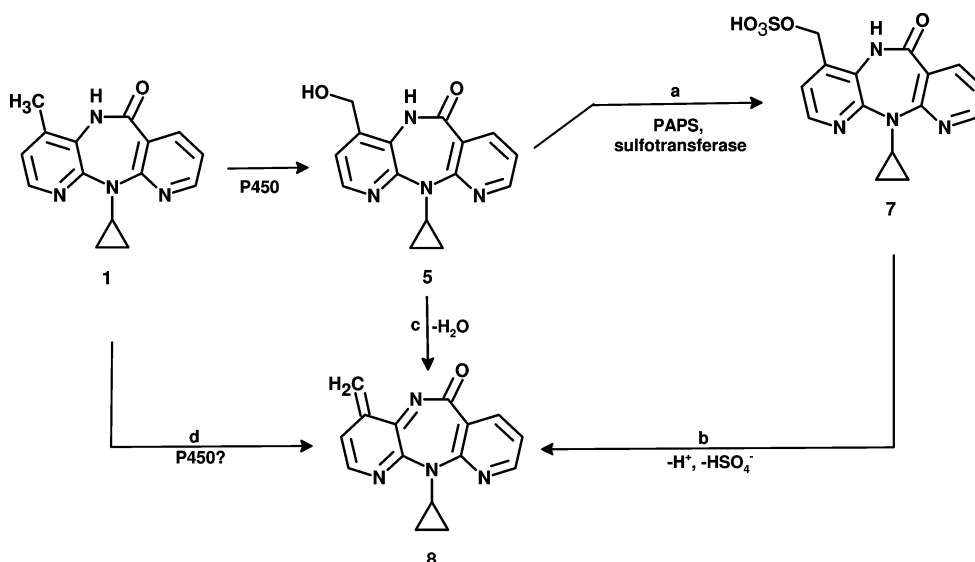
could generate reactive electrophiles potentially involved in the initiation of toxic events. Support for NVP sulfation in vivo has been provided by Chen et al. (21), who detected 12-sulfoxy-NVP (**7**) by LC-MS in urine and bile samples from female Brown Norway rats administered the parent drug. This rat strain and sex is particularly sensitive to an idiosyncratic NVP-induced skin rash that resembles the rash occurring in humans (22, 23). While both NVP and **5** induce the rash (21, 24), the lack of rash induction by 12-trideuteromethyl-NVP supports the involvement of **5** in the toxic response. The generation of a quinone methide intermediate (**8**, Scheme 1), possibly from **7**, was proposed as a factor in this process (21), although it may be argued that generation of a hapten adduct could stem from direct reaction of **7** with bionucleophiles. Nonetheless, the mass spectrometric detection of a putative 12-(glutathion-*S*-yl)-NVP (**10**) conjugate following incubation of NVP with human liver microsomes in the presence of glutathione (GSH) (25) suggests that NVP activation to the same quinone methide (**8**, Scheme 1) may occur without phase II conjugation, either by dehydration of **5** or by P450-induced dehydrogenation of NVP (Scheme 2). The formation of the NVP–GSH conjugate occurred following oxidation of NVP, primarily by P450 3A4 and to a lesser extent by P450 2D6, 2C19, and 2A6; moreover, the oxidation of NVP by P450 3A4 was found to cause a mechanism-based inactivation of the enzyme, which is consistent with the occurrence of covalent binding (25). A more recent study, screening for stable biomarkers of NVP bioactivation in rats and humans, has led to the identification of two NVP mercapturates, the major one through NVP-C3 and the minor one through NVP-C12, in the urine of HIV-positive patients administered NVP as part of a standard antiretroviral therapeutic regimen (26). The same conjugates were detected in the bile and urine of NVP-treated rats, as well as in incubations with rat hepatocytes and with rat and human liver microsomes supplemented with GSH or *N*-acetylcysteine (26).

Using 12-mesyloxy-NVP (**9**, Scheme 1) as a synthetic surrogate for the 12-sulfoxy metabolite of NVP, we have previously demonstrated that direct reaction of **9** with DNA in vitro yields a variety of covalent nucleoside and depurinating NVP–DNA adducts, consistently bound through the NVP C12 (27). Taking into consideration the potential role of covalent binding to skin proteins in the hypersensitivity reactions associated with NVP administration, we have further probed the utility of the model electrophile **9** by investigating its reaction with GSH and representative α -amino acids bearing nucleophilic side chains (cysteine, tryptophan, histidine, and arginine), as well as with the α -amino group of valine, whose adducted hydantoin derivatives are frequently used in biomonitoring studies as markers of binding to hemoglobin. We report herein the synthesis and characterization of a series of NVP–amino acid adduct standards and discuss their significance as potential biomarkers of NVP toxicity. A preliminary report of this work was presented at the 236th National Meeting of the American Chemical Society and published as an abstract (28).

Materials and Methods

Caution: NVP and its derivatives are potentially carcinogenic. They should be handled with protective clothing in a well-ventilated fume hood.

Chemicals. NVP was purchased from Cipla (Mumbai, India). All other commercially available reagents were acquired from Sigma-Aldrich Química, S.A. (Madrid, Spain) or Sigma Chemical Co. (St. Louis, MO) and used as received. (L)- α -Amino acids were used in all instances. Compounds **5** and **9** were prepared as

Scheme 2. Hypothetic Pathways for in Vivo Generation of the Putative Metabolite, NVP Quinone Methide (8)^a

^a Compound 5 is a known NVP metabolite in all species investigated. Evidence for the formation of 7 (represented in the neutral form) in vivo has been reported (21, 26); PAPS, 3'-phosphoadenosine-5'-phosphosulfate.

described in Antunes et al. (27). Whenever necessary, solvents were purified by standard methods (29).

Instrumentation. HPLC was conducted on an Ultimate 3000 Dionex system consisting of an LPG-3400A quaternary gradient pump and a diode array spectrophotometric detector (Dionex Co., Sunnyvale, CA) and equipped with a Rheodyne model 8125 injector (Rheodyne, Rohnert Park, CA). HPLC analyses were performed with a Luna C18 (2) column (250 mm × 4.6 mm; 5 μm; Phenomenex, Torrance, CA), at a flow rate of 1 mL/min. Semi-preparative HPLC separations were conducted with a Luna C18 (2) column (250 mm × 10 mm; 5 μm; Phenomenex) at a flow rate of 3 mL/min. The UV absorbance was monitored at 254 nm.

Mass spectra were recorded on either a ThermoFinnigan TSQ Quantum Ultra LC/MS system or a Varian 500-MS LC Ion Trap mass spectrometer, both operated in the electrospray ionization (ESI) mode. The samples were loaded onto a 5 μm Prodigy ODS(3) 100A column (250 mm × 2.0 mm; Phenomenex) or a 3 μm Gemini C18 column (150 mm × 2 mm; Phenomenex), and the mobile phase was delivered at a flow rate of 0.2 mL/min, using linear gradients from 5 or 10% acetonitrile up to 95% acetonitrile in 0.1% aqueous formic acid for durations between 15 and 40 min, depending on the specific sample.

¹H NMR spectra were recorded on a Bruker Avance III 400, a Bruker AV 500b, or a Bruker Avance III 600 (with cryoprobe) spectrometer, operating at 400, 500, and 600 MHz, respectively. ¹³C NMR spectra were recorded on the same instruments, operating at 100.62, 125.77, and 150.92 MHz, respectively. Chemical shifts are reported in ppm downfield from tetramethylsilane, and coupling constants (*J*) are reported in Hz; the subscripts *ortho*, *meta*, and *gem* refer to *ortho*, *meta*, and *geminal* couplings, respectively. Geminal protons are denoted with "a" and "b" subscripts, and asterisks are used to indicate a second conformer; the proton integrations listed below do not reflect the relative proportions of each conformer. The presence of labile protons was confirmed by chemical exchange with D₂O. Resonance and structural assignments were based on the analysis of coupling patterns, including the ¹³C–¹H coupling profiles obtained in bidimensional heteronuclear multiple bond correlation (HMBC) and heteronuclear multiple quantum coherence (HMQC) or heteronuclear single quantum coherence (HSQC)–total correlation spectroscopy (TOCSY) experiments, performed with standard pulse programs. A semiselective HMBC experiment was performed on the Bruker Avance III 600 (with cryoprobe) spectrometer, using a pulse program (shmbcgpndqf, available from the Bruker library) with no decoupling during acquisition and using gradient pulses for selection; excitation in ¹³C was ensured

by a 90° shaped sinc pulse (with 1 cycle and size shape 1000). ¹³C resonances were not discriminated whenever small sample quantities precluded the recording of one-dimensional ¹³C NMR spectra with good signal/noise ratios, despite having, for the most part, been detected in the inverse heteronuclear bidimensional experiments.

Syntheses. Reaction with GSH and *N*-Acetylcysteine. A solution of 9 (8 mg, 22 μmol) in THF (200 μL) was added to a solution of GSH or *N*-acetylcysteine (1.3 equiv, 29 μmol) in 1 mL of 50 mM phosphate buffer (pH 7.4). The reaction mixtures were incubated at room temperature for 2 h, and the products were purified by semipreparative HPLC using a 30 min linear gradient of 5–70% acetonitrile in 0.1% formic acid, followed by a 2 min linear gradient to 100% acetonitrile and a 16 min isocratic elution with acetonitrile.

12-(Glutathion-*S*-yl)-NVP (10). Compound 10 was obtained in 84% yield (10.6 mg); *t*_R, 14 min. UV, λ_{max} 292 nm. ¹H NMR [dimethyl sulfoxide (DMSO)-*d*₆]: δ 8.62 (1H, bs, Cys-NH), 8.50 (1H, d, *J*_{ortho} = 4.4, NVP-H9), 8.14 (1H, d, *J*_{ortho} = 4.8, NVP-H2), 8.04–8.02 (1H, m, NVP-H7), 7.89 (1H, bs, Gly-NH), 7.22–7.18 (2H, m, NVP-H8 + NVP-H3), 4.44–4.36 (1H, m, Cys-H2), 4.21 (1H, d, *J*_{gem} = 14.0, NVP-H12_a), 4.17 (1H, d, *J*_{gem} = 14.0, NVP-H12_a*), 3.77 (1H, d, *J*_{gem} = 14.0, NVP-H12_b), 3.75 (1H, d, *J*_{gem} = 14.0, NVP-H12_b*), 3.65–3.60 (1H, m, NVP-H13), 3.44–3.41 (2H, m, Gly-H2), 3.31 (1H, t, *J* = 6.0, Glu-H2), 2.81–2.72 (1H, m, Cys-H3_a), 2.61–2.57 (1H, m, Cys-H3_b), 2.32–2.29 (2H, m, Glu-H4), 1.92 (2H, bs, Glu-H3), 0.80–0.87 (2H, m, NVP-H14 + NVP-H15), 0.42–0.31 (2H, m, NVP-H14 + NVP-H15). ¹³C NMR (DMSO-*d*₆): δ 171.9 (Glu-C=O), 171.8 (Glu-C=O), 171.0 (Gly-C=O), 170.4 (Cys-C=O), 170.2 (Cys-C=O*), 167.1 (NVP-C6), 159.8 (NVP-C10a), 154.5 (NVP-C11a), 151.3 (NVP-C9), 143.7 (NVP-C2), 140.7 (NVP-C4), 140.6 (NVP-C4*), 140.0 (NVP-C7), 124.3 (NVP-C4a), 124.2 (NVP-C4a*), 121.3 (NVP-C8), 120.6 (NVP-C6a), 119.4 (NVP-C3), 53.1 (Glu-C2), 52.4 (Cys-C2), 52.3 (Cys-C2*), 41.4 (Gly-C2), 33.3 (Cys-C3), 33.0 (Cys-C3*), 31.4 (Glu-C4), 30.7 (NVP-C12), 30.5 (NVP-C12*), 29.3 (NVP-C13), 26.8 (Glu-C3), 8.7 (NVP-C14/C15), 8.4 (NVP-C14/C15). MS *m/z* 572 [MH]⁺, 443 [MH – pyroglutamate]⁺, 287 [MH₂]²⁺.

12-(*N*-Acetylcystein-*S*-yl)-NVP (11). Compound 11 was obtained in 82% yield (7.8 mg); *t*_R, 16 min. UV, λ_{max} 293 nm. ¹H NMR (acetone-*d*₆): δ 8.49 (1H, d, *J*_{ortho} = 3.9, NVP-H9), 8.15 (1H, d, *J*_{ortho} = 3.6, NVP-H2), 8.08 (1H, d, *J*_{ortho} = 6.2, NVP-

H7), 7.18–7.13 (2H, m, NVP-H8 + NVP-H3), 4.67 (1H, bs, Cys-H2), 4.21–3.91 (2H, m, NVP-H12), 3.72 (1H, bs, NVP-H13), 3.01–2.88 (2H, m, Cys-H3), 1.95 (3H, s, acetyl-CH₃), 0.86 (2H, bs, NVP-H14 + NVP-H15), 0.39 (2H, m, NVP-H14 + NVP-H15). ¹³C NMR (acetone-*d*₆): δ ca. 172 (Cys-C=O), 170.4 (acetyl C=O), 167.0 (NVP-C6), 161.2 (NVP-C10a), 155.7 (NVP-C11a), 152.5 (NVP-C9), 144.9 (NVP-C2), 141.0 (NVP-C7), 140.3 (NVP-C4), 140.1 (NVP-C4*), 125.7 (NVP-C4a), 125.6 (NVP-C4a*), 122.4 (NVP-C8), 121.5 (NVP-C6a), 119.9 (NVP-C3), 52.9 (Cys-C2), 34.5 (Cys-C3), 34.4 (Cys-C3*), 32.5 (NVP-C12), 32.3 (NVP-C12*), ca. 29.9 (NVP-C13, obscured by the solvent resonance), 22.7 (acetyl CH₃), 9.3 (NVP-C14/C15), 9.1 (NVP-C14/C15). MS *m/z* 428 [MH]⁺, 386 [MH₂ - COCH₃]⁺, 299 [MH₂ - CH₃CONHC(CH₂)CO₂H]⁺.

N-Deprotection of **11** (4 mg) was achieved by treatment with trifluoroacetic acid (970 μL) at 60 °C for 5 days. The reaction mixture was neutralized by addition of 10 M sodium hydroxide and analyzed by HPLC-MS. The hydrolysis reaction yielded 12-(cystein-*S*-yl)-NVP (**12**). MS *m/z* 386 [MH]⁺.

Reaction with Other Amino Acids. A solution of **9** (32 mg, 89 μmol) in THF (800 μL) was added to a solution of the amino acid (3.9 equiv, 350 μmol) in 4 mL of 50 mM phosphate buffer (pH 7.4). The reaction mixture was incubated at room temperature for 24 h, and the products were purified by semipreparative HPLC.

Reaction with Tryptophan. One adduct was isolated by semipreparative HPLC, using a 14 min linear gradient of 20–30% acetonitrile in 100 mM ammonium acetate (pH 5.7), followed by a 5 min linear gradient to 100% acetonitrile and a 10 min isocratic elution with acetonitrile. 12-(Tryptophan-2'-yl)-NVP (**13**) was obtained in 14% yield (5.7 mg); *t*_R, 13 min. UV, λ_{max} 220, 275, 282 nm. ¹H NMR (DMSO-*d*₆): δ 10.51 [1H, s, indole (Ind)-N1H], 10.42 (1H, s, Ind-N1H*), 8.48 (1H, dd, *J*_{ortho} = 4.7, *J*_{meta} = 1.9, NVP-H9), 8.44 (1H, dd *J*_{ortho} = 4.8, *J*_{meta} = 2.0, NVP-H9*), 8.11 (1H, d, *J*_{ortho} = 4.7, NVP-H2), 8.08 (1H, d, *J*_{ortho} = 4.9, NVP-H2*), 7.63–7.58 (2H, m, Ind-H7), 7.48 (2H, d, *J*_{ortho} = 7.3, NVP-H7 and NVP-H7*), 7.13–6.90 (10H, m, Ind-H4, H5, H6 + NVP-H3, H8; 2 isomers), 4.56–4.14 (4H, m, NVP-H12 + NVP-H12*), 3.63–3.59 (4H, m, NVP-H13 + NVP-H13* + Trp-H2 + Trp-H2*), ca. 3.33 (Trp-H3_a + Trp-H3_a*, obscured by the water resonance), 3.09 (1H, dd, *J*_{gem} = 15.0, ³*J* = 6.0, Trp-H3_b), 2.86 (1H, dd, *J*_{gem} = 14.6, ³*J* = 5.6, Trp-H3_b*), 0.90–0.84 (4H, m, NVP-H14 + NVP-H15 + NVP-H14* + NVP-H15*), 0.38–0.35 (4H, m, NVP-H14 + NVP-H15 + NVP-H14* + NVP-H15*). ¹³C NMR (DMSO-*d*₆): δ 172.7 (Trp-C1), 172.1 (Trp-C1*), 167.5 (NVP-C6), 167.1 (NVP-C6*), 160.3 (NVP-C10a), 160.2 (NVP-C10a*), 155.3 (NVP-C11a), 155.0 (NVP-C11a*), 151.5 (NVP-C9), 151.3 (NVP-C9*), 144.2 (NVP-C2), 143.9 (NVP-C2*), 143.1 (NVP-C4), 142.8 (NVP-C4*), 140.9 (NVP-C7), 140.7 (NVP-C7*), 136.1 (Ind-C7a), 133.8 (Ind-C2), 133.3 (Ind-C2*), 128.4 (Ind-C3a), 128.0 (Ind-C3a*), 124.7 (NVP-C4a), 124.5 (NVP-C4a*), 121.4, 120.9, 119.5, 119.4, 118.8, 118.6, 118.3, 118.2 (NVP-C3/C6a/C8; Ind-C4/C5/C6), 111.0 (Ind-C7), 110.9 (Ind-C7*), 109.1 (Ind-C3*), 108.2 (Ind-C3), 55.3 (Trp-C12), 29.5 (NVP-C13), 28.2 (NVP-C12), 28.0 (NVP-C12*), 26.9 (Trp-C3), 26.5 (Trp-C3*), 9.0 (NVP-C14/C15), 8.8 (NVP-C14/C15). MS *m/z* 469 [MH]⁺, 276 [MH₂ + 2CH₃CN]²⁺, 256 [MH₂ + CH₃CN]²⁺.

Reaction with *N*^α-*tert*-Butoxycarbonyl (Boc)-histidine. Two adducts were isolated using a 20 min linear gradient of 15–25% acetonitrile in 0.1% formic acid, followed by a 5 min linear gradient to 100% acetonitrile. 12-(*N*^α-Boc-histidin-*O*'-yl)-NVP (**14**) was obtained in 6% yield (2.5 mg) after further purification by preparative thin-layer chromatography [dichloromethane/methanol (10:1)]; *t*_R, 28 min. UV, λ_{max} 215, 295 nm. ¹H NMR

(DMSO-*d*₆): δ 10.06 (1H, s, NVP-N5H), 8.51 (1H, dd, *J*_{ortho} = 5.0, *J*_{meta} = 1.9, NVP-H9), 8.20 (1H, m, NVP-H2), 8.01 (1H, d, *J*_{ortho} = 7.5, NVP-H7), 7.58 [1H, bs, imidazole (Imid)-H2], 7.56 (1H, bs, Imid-H2*), 7.32 (<1H, bs, His-NH), 7.31 (<1H, bs, His-NH), 7.20 (1H, dd, *J*_{ortho} = 7.5, *J*_{ortho}' = 5.0, NVP-H8), 7.07–7.04 (1H, m, NVP-H3), 6.84 (1H, m, Imid-H5), 6.79 (1H, m, Imid-H5*), 5.34–5.17 (2H, m, NVP-H12), 4.36–4.31 (1H, m, Hist-H2), 3.66–3.62 (1H, m, NVP-H13), 2.92–2.85 (2H, m, Hist-H3), 1.36 (9H, s, Boc-CH₃), 0.92–0.85 (2H, m, NVP-H14 + NVP-H15), 0.42–0.32 (2H, m, NVP-H14 + NVP-H15). ¹³C NMR (DMSO-*d*₆): δ 172.3 (Hist-C=O), 167.5 (NVP-C6), 160.1 (NVP-C10a), 155.8 (Boc-C=O), 155.1 (NVP-C11a), 151.9 (NVP-C9), 144.4 (NVP-C2), 140.6 (NVP-C7), 138.9 (NVP-C4), 135.6 (Imid-C2/Imid-C4), 135.5 (Imid-C2/Imid-C4), 123.6 (NVP-C4a), 121.3 (NVP-C6a), 119.9 (NVP-C8), 118.8 (NVP-C3), 116.9 (Imid-C5), 78.9 (Boc-C-O), 62.0 (NVP-C12), 54.5 (Hist-C2), 29.4 (NVP-C13), 29.1 (Hist-C3), 28.5 (Boc-CH₃), 9.2 (NVP-C14/C15), 8.9 (NVP-C14/C15). MS *m/z* 520 [MH]⁺, 420 [MH₂ - Boc]⁺, 302 [MH₂ + 2CH₃CN]²⁺, 281 [MH₂ + CH₃CN]²⁺, 261 [MH₂]²⁺, 253 [MH + 2H + CH₃CN - *tert*-butyl (*t*-Bu)]²⁺. 12-(*N*^α-Boc-histidin-*N*'-yl)-NVP (**15**) was obtained in 13% yield (5.9 mg); *t*_R, 24 min. UV, λ_{max} 216, 297 nm. ¹H NMR (DMSO-*d*₆): δ 10.16 (1H, bs, His-CO₂H), 8.49 (1H, d, *J* = 3.3, NVP-H9), 8.29 (<1H, bs, NH), 8.08 (1H, d, *J* = 4.7, NVP-H2), 7.98 (1H, d, *J*_{ortho} = 7.2, NVP-H7), 7.59 (1H, s, Imid-H2), 7.19 (1H, dd, *J*_{ortho} = 7.4, *J*_{ortho}' = 4.8, NVP-H8), 6.84 (1H, bs, Imid-H5), 6.76 (1H, bs, NH), 6.32–6.29 (1H, m, NVP-H3), 5.33 (1H, bs, NVP-H12), 4.02 (1H, bs, Hist-H2), ca. 3.40 (NVP-H13, obscured by the water resonance), 2.87–2.76 (2H, m, Hist-H3), 1.28 (9H, s, Boc-CH₃), 0.86–0.85 (2H, m, NVP-H14 + NVP-H15), 0.36–0.22 (2H, m, NVP-H14 + NVP-H15). ¹³C NMR (DMSO-*d*₆): δ 174.3 (His-C=O), 167.6 (NVP-C6), 160.2 (NVP-C10a), 155.6 (Boc-C=O), 155.1 (NVP-C11a), 151.9 (NVP-C9), 144.7 (NVP-C2), 141.2 (NVP-C4), 140.5 (NVP-C7), 138.9 (Imid-C4), 137.9 (Imid-C2), 123.5 (NVP-C4a), 121.3 (NVP-C6a), 120.0 (NVP-C8), 118.3 (NVP-C3), 118.1 (Imid-C5), 78.2 (Boc-C-O), 54.4 (Hist-C2), 45.7 (NVP-C12), 30.6 (Hist-C3), 29.8 (NVP-C13), 28.6 (Boc-CH₃), 9.2 (NVP-C14/C15), 8.9 (NVP-C14/C15). MS *m/z* 520 [MH]⁺, 281 [MH₂ + CH₃CN]²⁺, 261 [MH₂]²⁺, 253 [MH + 2H + CH₃CN - *t*-Bu]²⁺.

Reaction with Histidine. One adduct was isolated by semipreparative HPLC, using a 30 min linear gradient of 5–30% acetonitrile in 100 mM ammonium acetate (pH 5.7), followed by a 5 min linear gradient to 100% acetonitrile and a 10 min isocratic elution with acetonitrile. 12-(Histidin-*N*'-yl)-NVP (**16**) was obtained in 10% yield (3.7 mg); *t*_R, 19.5 min. UV, λ_{max} 215, 288 nm. ¹H NMR (DMSO-*d*₆): δ 10.23 (1H, bs, NVP-N5H), 8.52 (1H, bs, NVP-H9), 8.15 (1H, bs, NVP-H2), 8.01 (1H, m, NVP-H7), 7.68 (1H, bs, Imid-H2), ca. 7.25 (bs, His-NH₂), 7.23–7.18 (1H, m, NVP-H8), 7.00 (1H, bs, NVP-H3), 6.98 (1H, bs, NVP-H3*), 6.54 (1H, bs, Imid-H5), 5.44–5.38 (2H, m, NVP-H12), 3.63 (1H, bs, NVP-H13), ca. 3.40 (Hist-H2, obscured by the water resonance), 3.05–3.03 (1H, m, Hist-H3_a), 2.73 (1H, bs, Hist-H3_b), 0.88 (2H, bs, NVP-H14 + NVP-H15), 0.40–0.33 (2H, m, NVP-H14 + NVP-H15). MS *m/z* 420 [MH]⁺, 231 [MH₂ + CH₃CN]²⁺, 211 [MH₂]²⁺.

Reaction with Arginine. One adduct was isolated by semipreparative HPLC, using a 14 min linear gradient of 15–70% acetonitrile in 100 mM ammonium acetate (pH 5.7), followed by a 5 min linear gradient to 100% acetonitrile. 12-(Arginin-*N*^ε-yl)-NVP (**17**) was obtained in 6% yield (2.4 mg); *t*_R, 8 min. UV, λ_{max} 216, 240, 302 nm. ¹H NMR (DMSO-*d*₆): δ 9.06 (2H, bs, NH), 8.52 (2H, bs, NVP-H9 + NVP-H9*), 8.12 (2H, bs, NVP-H2 + NVP-H2*), 8.05–8.02 (2H, m, NVP-H7 + NVP-H7*), 7.93 (4H, bs, NH), 7.19 (2H, bs, NVP-H8 + NVP-H8*), 7.12–7.11 (2H, m, NVP-H3 + NVP-H3*), 3.88–3.57 (6H, m, NVP-H12 + NVP-H12* + NVP-H13 + NVP-H13*), 3.05–3.01 (4H, m, Arg-H5 + Arg-

H5*), 2.91 (1H, bs, Arg-H2), 2.76 (1H, bs, Arg-H2*), 1.61–1.48 (8H, m, Arg-H3 + Arg-H3* + Arg-H4 + Arg-H4*), 0.88–0.85 (4H, bs, NVP-H14 + NVP-H14* + NVP-H15 + NVP-H15*), 0.37–0.31 (4H, m, NVP-H14 + NVP-H14* + NVP-H15 + NVP-H15*). ¹³C NMR (DMSO-*d*₆): δ 173.3 (Arg-C1), 166.5 (NVP-C6), 166.3 (NVP-C6*), 159.9 (NVP-C10a), 159.8 (NVP-C10a*), 157.4 (guanidine-C + guanidine-C*), 153.0 (NVP-C11a + NVP-C11a*), 151.4 (NVP-C9 + NVP-C9*), 144.2 (NVP-C2), 144.0 (NVP-C2*), 142.9 (NVP-C4), 142.7 (NVP-C4*), 140.7 (NVP-C7), 140.4 (NVP-C7*), 126.0 (NVP-C4a + NVP-C4a*), 121.9 (NVP-C3), 120.9 (NVP-C3*), 120.0 (NVP-C6a + NVP-C6a*), 118.8 (NVP-C8 + NVP-C8*), 62.2 (Arg-C2), 61.3 (Arg-C2*), 50.3 (NVP-C12 + NVP-C12*), 42.0 (Arg-C5 + Arg-C5*), 30.1 (Arg-C3 + Arg-C3*), 28.9 (NVP-C13 + NVP-C13*), 25.8 (Arg-C4 + Arg-C4*), 8.9 (NVP-C14/C15), 8.6 (NVP-C14*/C15*), 7.8 (NVP-C14/C15), 7.6 (NVP-C14*/C15*). MS *m/z* 439 [MH]⁺, 241 [MH₂ + CH₃CN]²⁺, 220 [MH₂]²⁺.

Reaction with Ethyl Valinate. One adduct was isolated by semipreparative HPLC, using a 30 min linear gradient of 5–70% acetonitrile in 0.1% formic acid. 12-(Ethyl valinate-*N*^α-yl)-NVP (**18**) was obtained in 33% yield (12.0 mg); *t*_R, 27.6 min. UV, λ_{max} 239, 294 nm. ¹H NMR (MeOD): δ 8.51–8.50 (2H, m, NVP-H9 + NVP-H9*), 8.14 (4H, bs, NVP-H2 + NVP-H2* + NVP-H7 + NVP-H7*), 7.19–7.18 (2H, m, NVP-H8 + NVP-H8*), 7.12–7.11 (2H, m, NVP-H3 + NVP-H3*), 4.26–4.17 (4H, m, Val-OCH₂CH₃ + Val-OCH₂CH₃*), 4.11 (1H, d, *J*_{gem} = 13.8, NVP-H12a), 3.82 (2H, s, NVP-H12a* + NVP-H12b*), 3.73 (2H, bs, NVP-H13 + NVP-H13*), 3.63 (1H, d, *J*_{gem} = 13.8, NVP-H12b), 3.32–3.00 (1H, m, Val-H2*), 2.87–2.71 (1H, m, Val-H2), 2.07–2.02 (1H, m, Val-H3*), 1.99–1.95 (1H, m, Val-H3), 1.32–1.27 (6H, Val-OCH₂CH₃ + Val-OCH₂CH₃*), 1.18–1.03 (6H, m, Val-CH₃a* + Val-CH₃b*), 0.96–0.89 (10H, m, Val-CH₃a + Val-CH₃b + NVP-H14/H15 + NVP-H14/H15*), 0.47–0.36 (4H, m, NVP-H14/H15 + NVP-H14/H15*). ¹³C NMR (MeOD): δ 174.0 (Val-C1/C1*), 173.9 (Val-C1/C1*), 167.4 (NVP-C6 + NVP-C6*), 159.9 (NVP-C10a + NVP-C10a*), 151.6 (NVP-C9 + NVP-C9*), 143.6 (NVP-C2 + NVP-C2*), 140.3 (NVP-C7 + NVP-C7*), 139.1 (NVP-C4 + NVP-C4*), 126.0 (NVP-C4a + NVP-C4a*), 121.5 (NVP-C3*), 120.9 (NVP-C3), 119.1 (NVP-C8 + NVP-C8*), 67.4 (Val-OCH₂CH₃*), 65.4 (Val-OCH₂CH₃), 60.5 (Val-C2), 60.4 (Val-C2*), 50.1 (NVP-C12*), 48.8 (NVP-C12), 31.4 (Val-C3/Val-C3*), 31.1 (Val-C3/Val-C3*), 29.1 (NVP-C13 + NVP-C13*), 18.6 (Val CH₃a/CH₃b/CH₃a*/CH₃b*), 18.4 (Val CH₃a/CH₃b/CH₃a*/CH₃b*), 17.6 (Val CH₃a/CH₃b/CH₃a*/CH₃b*), 17.3 (Val CH₃a/CH₃b/CH₃a*/CH₃b*), 13.3 (Val-OCH₂CH₃/Val-OCH₂CH₃*), 13.2 (Val-OCH₂CH₃/Val-OCH₂CH₃*), 8.4 (NVP-C14/C15/C14*/C15*), 8.1 (NVP-C14/C15/C14*/C15*). MS *m/z* 432 [MH + Na]⁺, 410 [MH]⁺, 265 [MH + ethyl valinate]⁺.

O-Deprotection of **18** (5.0 mg, in 1 mL of methanol) was achieved by treatment with 1 M KOH (200 μL). The solution was stirred at 40 °C and periodically monitored by HPLC until completion (72 h). Following neutralization with HCl, the hydrolysate yielded a single product, which was purified by semipreparative HPLC. 12-(Valin-*N*^α-yl)-NVP (**19**) was obtained in 86% yield (4.0 mg); *t*_R, 12.7 min. UV, λ_{max} 238, 302 nm. ¹H NMR (DMSO-*d*₆): δ 10.51 (1H, s, NVP-N5H), 8.52–8.51 (2H, d, NVP-H9 + NVP-H9*), 8.14–8.13 (2H, m, NVP-H2 + NVP-H2*), 8.03–8.02 (2H, m, NVP-H7 + NVP-H7*), 7.20–7.18 (2H, m, NVP-H8 + NVP-H8*), 7.12–7.09 (2H, m, NVP-H3 + NVP-H3*), 4.01 (1H, d, *J*_{gem} = 14.3, NVP-H12a), 3.80 (1H, d, *J*_{gem} = 13.8, NVP-H12a*), 3.70 (1H, d, *J*_{gem} = 13.8, NVP-H12b*), 3.64–3.60 (2H, m, NVP-H13 + NVP-H13*), 3.56 (1H, d, *J*_{gem} = 14.3, NVP-H12b), 2.89 (1H, d, *J* = 5.5, Val-H2*), 2.60 (1H, d, *J* = 5.4, Val-H2), 1.94–1.84 (2H, m, Val-H3 + Val-H3*), 0.98 (3H, d, *J* = 6.7, Val-CH₃a), 0.92 (3H, d, *J* = 6.7, Val-CH₃b), 0.86–0.81 (10H, m, Val-CH₃a* + Val-CH₃b* + NVP-H14/H15 + NVP-H14/H15*), 0.37–0.26 (4H, m, NVP-H14/H15 + NVP-H14/H15*). ¹³C NMR (DMSO-*d*₆): δ 171.0 (Val-C1 + Val-C1*), 164.5 (NVP-C6 + NVP-C6*), 159.7 (NVP-C10a + NVP-C10a*), 151.6 (NVP-C9 + NVP-C9*), 143.4 (NVP-C2 + NVP-C2*), 140.2 (NVP-C7 + NVP-C7*), 140.1 (NVP-C4 + NVP-C4*), 125.8 (NVP-C4a + NVP-C4a*), 119.4

(NVP-C8 + NVP-C8*), 67.5 (Val-C2*), 65.9 (Val-C2), 49.7 (NVP-C12*), 48.5 (NVP-C12), 30.8 (Val-C3/Val-C3*), 30.5 (Val-C3/Val-C3*), 29.5 (NVP-C13 + NVP-C13*), 20.0 (Val-CH₃a*), 19.6 (Val CH₃a), 18.4 (Val CH₃b/CH₃b*), 18.2 (Val CH₃b/CH₃b*), 8.9 (NVP-C14/C15 + NVP-C14/C15*), 8.6 (NVP-C14/C15 + NVP-C14/C15*). MS *m/z* 382 [MH]⁺, 336 [MH – HCO₂H]⁺, 282 [NVP-NH₂ + H]⁺, 265 [MH – valine]⁺.

Preparation of an *N*-Alkyl Edman Derivative from **18.** 12-[5-Isopropyl-4-oxo-3-phenyl-2-thioxoimidazolidin-1-yl]-NVP (**20**). The thiohydantoin derivative was prepared by treatment of **18** (5.0 mg, 12 μmol) with phenyl thioisocyanate (1.4 μL, 12 μmol) in dioxane (1 mL), in the presence of 1 M KOH (10 μL). The reaction mixture was stirred for 3 h at 55 °C, and the product was purified by semipreparative HPLC using a 20 min linear gradient of 5–52% acetonitrile in 0.1% formic acid, followed by a 5 min linear gradient to 100% acetonitrile and a 2 min isocratic elution with acetonitrile. The thiohydantoin **20** was obtained in 13% yield (0.8 mg); *t*_R, 27.9 min. UV, λ_{max} 218, 236, 266 nm. ¹H NMR (CDCl₃): δ 9.12 (1H, s, NVP-N5H), 8.55 (2H, bs, NVP-H9 + NVP-H9*), 8.30 (2H, bs, NVP-H2 + NVP-H2*), 8.13 (2H, d, *J* = 7.4, NVP-H7), 8.08 (1H, d, *J* = 7.3, NVP-H7*), 7.56–7.28 [10H, m, phenyl (Ph)-H + Ph-H*], 7.08–7.07 (2H, m, NVP-H8 + NVP-H8*), 7.01–6.94 (2H, m, NVP-H3 + NVP-H3*), 6.27 (1H, d, *J*_{gem} = 16.4, NVP-H12a), 5.72 (1H, d, *J*_{gem} = 15.4, NVP-H12a*), 4.61 (1H, d, *J*_{gem} = 15.4, NVP-H12b*), 4.43 (1H, d, *J*_{gem} = 16.4, NVP-H12b), 4.11 (1H, bs, hydantoin-H5), 3.78 (2H, bs, NVP-H13 + NVP-H13*), 3.62 (1H, bs, hydantoin-H5*), 2.55–2.49 (1H, m, isopropyl-CH), 2.32–2.27 (1H, m, isopropyl-CH*), 1.30 (3H, d, *J* = 6.6, CH₃a), 1.11 (3H, d, *J* = 6.4, CH₃b), 1.00–0.99 (10H, m, CH₃a* + CH₃b* + NVP-H14/H15 + NVP-H14/H15*), 0.63–0.43 (4H, m, NVP-H14/H15 + NVP-H14/H15*). MS *m/z* 499 [MH]⁺, 265 [MH – C₁₂H₁₄N₂OS]⁺.

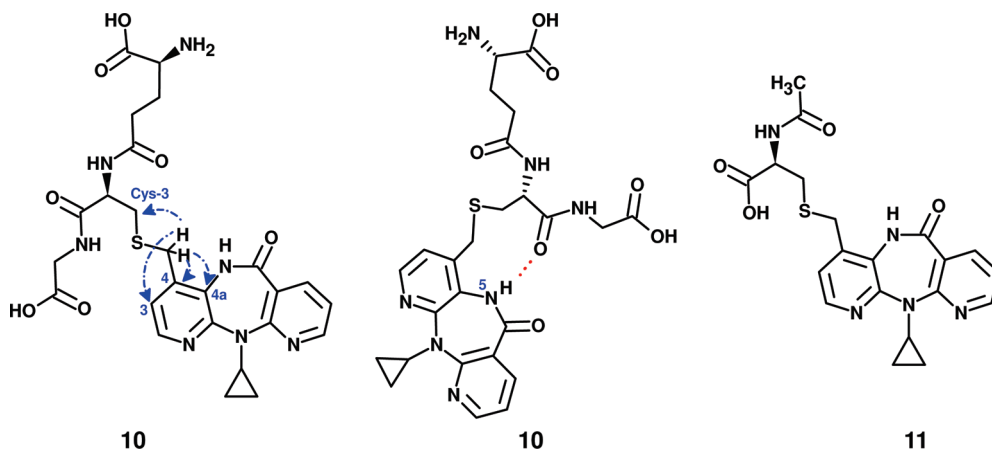
Computational Methods. All species were drawn and preoptimized using a Dreiding type molecular mechanics force field (30), implemented in the Marvin software and the Calculator plug-ins (31). Calculations were performed with the Parametrized Model 6 (32) as implemented in MOPAC2009 (33), using a Conductor-like Screening Model (COSMO) method to approximate the effect of the solvent; DMSO was used for the calculations. In all instances, geometry optimization was terminated when the gradient dropped below 0.01. PM6DH (34), which adds correction terms for PM6 to reflect noncovalent interactions, such as hydrogen bonding, was also used to fine-tune further the calculated geometries and energies. All values are in kJ/mol.

Results and Discussion

We have previously demonstrated DNA adduct formation *in vitro* by **9**, used as a surrogate for the phase II NVP metabolite, **7**. To address the potential involvement of NVP–protein binding in the toxic events associated with NVP administration, the availability of reliable NVP–amino acid adduct standards is essential. To gain insight into potentially reactive sites in proteins and prepare fully characterized NVP–amino acid adduct standards for subsequent assessment as biomarkers of NVP toxicity, we have investigated the reaction of **9** with the tripeptide GSH, ethyl valinate, and selected α-amino acids containing nucleophilic side chains.

Preliminary experiments, conducted to establish the most suitable reaction conditions, demonstrated a correlation between the extent of adduct formation and the anticipated nucleophilicity of the amino acids (e.g., S > N), as expected for a bimolecular mechanism. HPLC analyses of the reaction mixtures indicated that the only additional product was, in all instances, the hydrolysis product, **5**, which was identified by comparison with a synthetic standard (27).

The optimized reactions were typically conducted at room temperature in 50 mM phosphate buffer (pH 7.4)/THF (5:1) using a 3.9 molar excess of the nucleophile, with the exception

Scheme 3. Structures of **10** and **11**, Obtained in the Reaction of **9** with GSH and *N*-Acetylcysteine, Respectively^a

^a The arrows in structure **10** (on the left) represent the HMBC correlations of the NVP-H12 protons with specific NVP and GSH carbons. For simplicity, arrows are drawn from only one of the geminal NVP protons, although both exhibited correlations to the same carbons. The middle structure displays a hydrogen bond [(NVP)N5H \cdots O=C(Cys)], present in the lowest energy conformer obtained by theoretical simulation of adduct **10** in DMSO at 298 K.

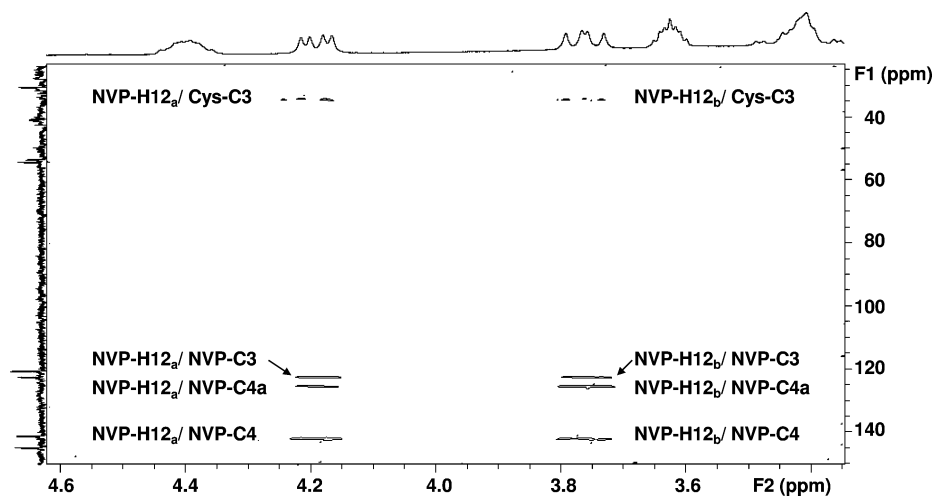
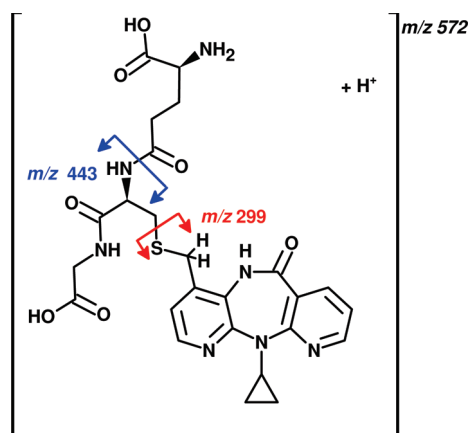


Figure 1. Expanded region of the ^1H – ^{13}C HMBC spectrum of **10**, displaying the connectivities between the geminal NVP-H12 protons and the carbons of the NVP (C3, C4, and C4a) and GSH (Cys-C3) moieties. The three-bond connectivity with the Cys-3 carbon was decisive to assign the cysteine sulfur as the binding site in GSH.

of the thionucleophiles, GSH and *N*-acetylcysteine, for which a 1.3 molar excess proved to be sufficient for a significant adduct yield. In each instance, NVP–amino acid adducts were isolated by semipreparative reversed-phase HPLC and fully characterized by ^1H and ^{13}C NMR spectroscopy and mass spectrometry; all of the isolated adducts consistently involved binding through the C12 position of NVP. The binding regioselectivity was expressed unequivocally in the ^1H NMR and ^{13}C NMR spectra of the isolated adducts, which showed all of the expected NVP and amino acid signals, and by the resonances of the two geminal H12 NVP protons (as well as the C12 carbon), which were strongly dependent on the nature of the amino acid atom establishing the connectivity to the NVP fragment. Further confirmation of the binding position was achieved for each adduct through observation of three-bond ^1H – ^{13}C correlations displayed in the HMBC spectra between the NVP H12 protons and the relevant carbons of the amino acid moiety.

As implied above, the thionucleophiles GSH and *N*-acetylcysteine were the most reactive. Thus, using a slight (1.3 equiv) molar excess of the nucleophile and a short incubation time (2 h), the adducts **10** (Scheme 3) and **11** (Scheme 3) were isolated in 84 and 82% yield, respectively. The ^1H (Figure S1 of the Supporting Information) and ^{13}C NMR spectra of **10** showed all of the expected resonances from both the GSH and the NVP

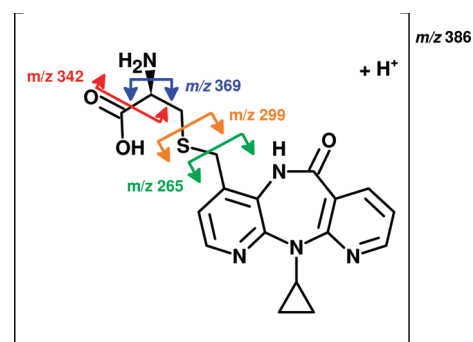
moieties. The assignment of all ^1H NMR and ^{13}C NMR resonances was based on the correlations observed in both HSQC-TOCSY and HMBC spectra (not shown). Evidence for the connectivity through the NVP C12 position was initially obtained from the ^1H NMR spectrum, where the signals from the H12 protons appeared as duplicate (vide infra) sets of two double duplets (at 3.75, 3.77, 4.17, and 4.21 ppm), each accounting for one proton, with a geminal coupling constant of 14 Hz as clear evidence of magnetic anisotropy. Furthermore, the location of the H12 (resonances indicated above) and C12 (30.5 and 30.7 ppm) NVP resonances was consistent with a methylene bridge between the aromatic moiety and a sulfur atom. This connectivity was unequivocally confirmed with the HBMBC correlations established by the geminal NVP H12 protons; thus, in addition to the expected two- and three-bond interactions to carbons of the NVP moiety (C3, C4, and C4a), a correlation was found with the C3 of the cysteine residue in GSH at 33.0 and 33.3 ppm (Scheme 3 and Figure 1). Similarly to the NVP H12 protons, the NVP C4, C4a, and C12 and the cysteine C1, C2, and C3 (in the GSH fragment) had duplicate resonances, which suggested restricted rotational mobility between the GSH and the NVP moieties. Further confirmation of covalent binding between the NVP and the GSH moieties was obtained from the LC/ESI-MS spectrum of **10** (not shown),

Scheme 4. ESI-MS/MS Fragmentation Pattern for the Protonated Molecule (m/z 572) of **10**

which displayed the protonated molecule at m/z 572, a fragment ion resulting from loss of pyroglutamate at m/z 443, and a base peak (m/z 287) corresponding to the diprotonated molecule. Moreover, the ESI-tandem mass spectrometry (MS/MS) spectrum of MH^+ showed a daughter ion at m/z 299 [(NVP + S + H) $^+$], stemming from cleavage of the S–C3 bond of the cysteine residue in GSH, with the sulfur remaining attached to the NVP moiety (Scheme 4). The same fragment ion was observed by Wen et al. (25) for an NVP–GSH conjugate obtained in incubations of NVP with human liver microsomes supplemented with GSH and was assumed to involve binding through the NVP C12, but definite proof of the site of attachment was not provided. Likewise, although Srivastava et al. (26) reported the detection of **10** in the bile of NVP-treated rats and in incubations of NVP with rat hepatocytes, the structural evidence was based upon the m/z 572 \rightarrow 443 transition in the MS/MS spectrum, and the binding position was inferred from indirect evidence only.

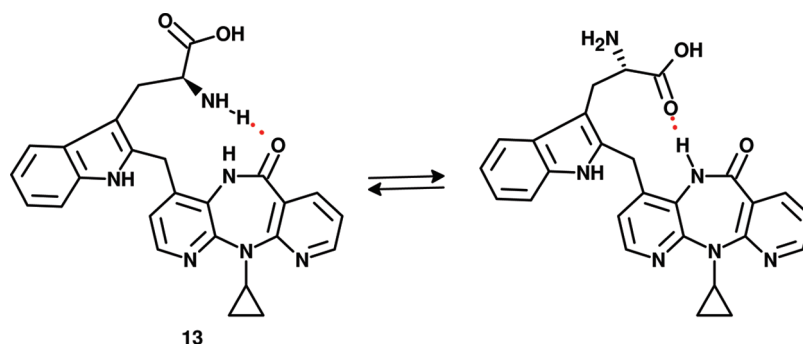
Using PM6DH, which includes solvation, we calculated enthalpies of formation for adduct **10** considering numerous possibilities of hydrogen bond formation. The calculations were conducted assuming a temperature of 298 K and ignoring pK_a effects, by working with nonionized molecules. The computations yielded a large number of low energy conformers, of which the most stable (by ca. 11 kJ/mol) had an intramolecular hydrogen bond between the NVP N5H and the carbonyl oxygen of the cysteine residue in GSH (Scheme 3). Despite the simplifications of the model, this result is consistent with the detection of different conformers of **10** in DMSO solution. In fact, the RT parameter is approximately 2.5 kJ/mol at 298 K, which suggests that thermal motion is insufficient to allow free interconversion at room temperature.

The 1H NMR (Figure S2 of the Supporting Information) and ^{13}C NMR spectra of the *N*-acetylcysteine–NVP adduct (**11**) showed all of the signals expected from the NVP and amino acid moieties. Although we were unable to detect a three-bond 1H – ^{13}C correlation between the NVP H12 protons and the cysteine C3 in the HMBC spectrum, the occurrence of nucleophilic attack by the thiol group of cysteine at the C-12 position of NVP is consistent with the MS data. Thus, as observed for **10**, the MS/MS spectrum of the protonated molecule (m/z 428) showed a daughter ion at m/z 299 stemming from cleavage of the S–C3 bond of cysteine, with the sulfur remaining attached to the NVP moiety. In addition, similarly to the GSH–NVP adduct, the ^{13}C NMR spectrum of **11** showed evidence for the presence of two conformers, as indicated by duplication of the signals for the NVP C12 (32.3 and 32.5 ppm) and the cysteine

Scheme 5. ESI-MS/MS Fragmentation Pattern for the Protonated Molecule (m/z 386) of **12**

C3 (34.4 and 34.5 ppm). The sensitivity of these specific carbons to conformational effects is entirely consistent with binding through the NVP C12. The observation of comparable, and relatively shielded, resonances for the NVP C12 in adducts **10** (30.5 and 30.7 ppm) and **11** (vide supra) provides further confirmation of the binding site. *N*-Deacetylation of adduct **11** was achieved by treatment with trifluoroacetic acid at 60 °C. Following neutralization, HPLC-MS analysis of the reaction mixture indicated the presence of adduct **12** (Scheme 5). MS/MS of the protonated molecule (m/z 386), using a 0.9 V excitation energy, yielded characteristic fragment ions at m/z 369 ($MH^+ - NH_3$), m/z 342 ($MH^+ - CO_2$), and m/z 265 ($MH^+ - \text{cysteine}$); the base peak, observed at m/z 299 ($MH^+ - C_3H_5NO_2$), corresponded to the already identified [(NVP + S + H) $^+$] fragment (Scheme 5). The *N*-acetylated adduct **11** was identified by Srivastava et al. (26) as one of the two NVP mercapturates (designated NVP-M1) detected in the bile and urine of NVP-treated rats, in human urine, and in incubations of NVP with rat hepatocytes. Their structural evidence relied on the 428 \rightarrow 299 MS/MS fragmentation and on the 1H NMR spectrum of a very diluted sample, recorded in deuterated methanol and presented in graphic form. The authors based the assignment of the NVP binding site on the observation of all of the aromatic NVP signals and of an NOE cross-peak between the H3 and the H12 protons of NVP. It is not clear whether this NOE signal was properly identified since, judging from the figure labels, the authors mistook a very weak signal at ca. 3.55 ppm for the signal of the NVP H12 protons, while missing two apparent doublets of proper intensity at ca. 3.8 and 4.0 ppm, having the characteristic pattern of nonequivalent geminal protons. Nonetheless, despite the limitations of visual inspection and slight variations associated with the use of different solvents, the 1H NMR spectrum displayed by Srivastava et al. (26) for NVP-M1 is consistent with our data for the synthetic adduct **11**.

Reaction with tryptophan resulted in the formation of **13** (Scheme 6) in 14% yield. Both the 1H NMR and the ^{13}C NMR spectra were rather complex, due to the existence of duplicate resonances. Simplification of some 1H NMR signals was observed upon heating from 25 to 70 °C (Figure 2), which suggests that the sample consisted of a mixture of two readily interconvertible conformers, having comparable populations at room temperature. The same theoretical methodology applied for adduct **10** indicated a variety of low energy conformers for structure **13**, of which the two more stable isomers (Scheme 6) differed by only 3.2 kJ/mol and were considerably more stable (by at least 8 kJ/mol) than any other conformer. Again, despite the approximations involved, these results are consistent with the interconversion observed in the 1H NMR spectrum at a relatively low temperature. Evidence for adduct formation

Scheme 6. Structure of 13, Obtained in the Reaction of 9 with Tryptophan^a

^a The adduct is shown as two different conformers in equilibrium. Theoretical simulation of **13** in DMSO at 298 K indicated a difference of 3.24 kJ/mol between the lowest energy conformer, having a (Trp)N¹H \cdots O=C6(NVP) hydrogen bond (left), and the next more stable conformer, having a (Trp)C1=O \cdots HN5(NVP) hydrogen bond (right).

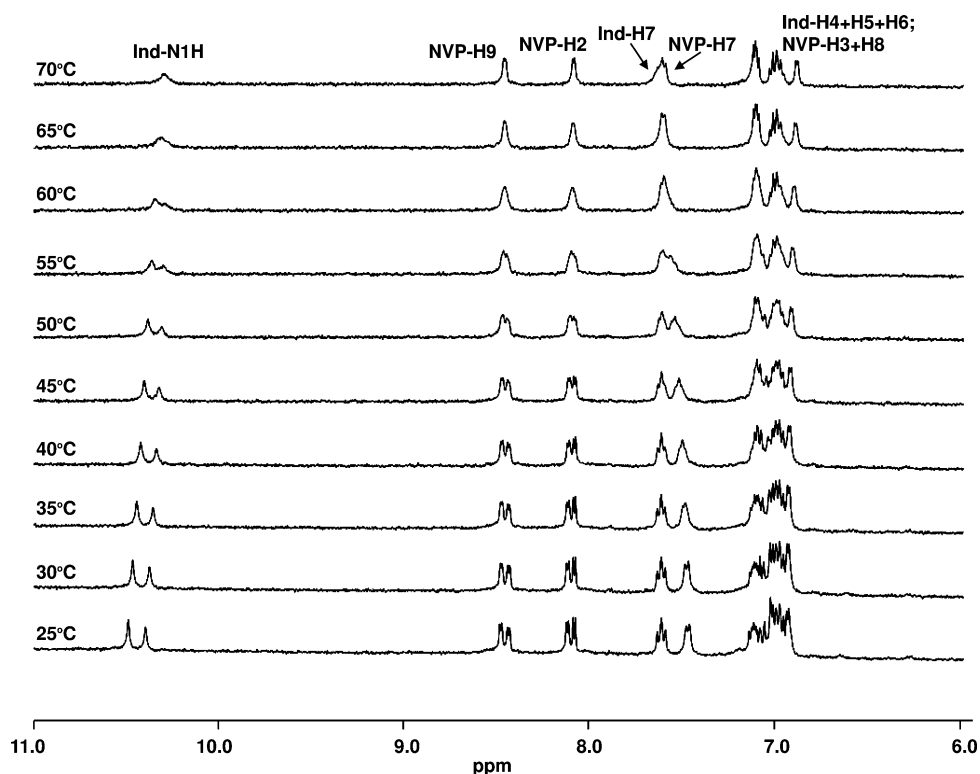


Figure 2. Expanded downfield region of the ¹H NMR spectrum of **13**, recorded in DMSO-*d*₆ as a function of temperature, showing the gradual collapse of duplicate resonances upon heating. The observed changes were reversible on cooling to room temperature.

through C2 of the Ind ring of tryptophan was first obtained from the ¹H NMR spectrum, which showed signals in the downfield region accounting for all of the aromatic NVP protons but where one of the aromatic Ind protons was missing. Furthermore, two singlets at 10.42 and 10.51 ppm were unequivocally ascribed to the exchangeable N1H protons of the Ind ring in each rotamer, since HMBC correlations (not shown) were observed between these protons and the Ind-C2 (133.3 and 133.8 ppm), Ind-C3 (108.2 and 109.1 ppm), and Ind-C3a (128.0 and 128.4 ppm); this observation excluded binding of the NVP moiety through N1 of the Ind ring. Moreover, the ¹³C NMR spectrum showed that both rotamers had a relatively shielded NVP C12 (28.0 and 28.2 ppm), when compared to all other NVP adducts characterized in this study (Table 1), which involved binding of the NVP C12 to heteroatoms in the amino acid residue and to the resonances observed for **5** (59.3 ppm) and **9** (66.0 ppm) (27); this is entirely consistent with direct connectivity to a less deshielding carbon atom. To obtain definite structural proof, and because no correlations between the geminal NVP H12

Table 1. Comparison of the ¹³C NMR Resonances for C12 of the NVP Fragment^a

Compound	C12–O bond	C12–N bond	C12–S bond	C12–C bond
5	59.3 ^b			
9	66.0 ^{b,c}			
10			30.5, 30.7 ^d	
11			32.3, 32.5 ^{d,e}	
13				28.0, 28.2 ^d
14	62.0			
15		45.7		
17		50.3		
19		48.5, 49.7 ^d		

^a Unless indicated, the spectra were recorded in DMSO-*d*₆. Chemical shifts are in ppm, downfield from tetramethylsilane. ^b Data from ref 27. ^c Recorded in CDCl₃. ^d Two conformers were detected. ^e Recorded in acetone-*d*₆.

protons and any Ind carbons were detected in the standard HMBC spectrum, a semiselective HMBC experiment was performed to enhance the spectral resolution, using a shaped pulse for excitation and a gradient pulse for selection. The

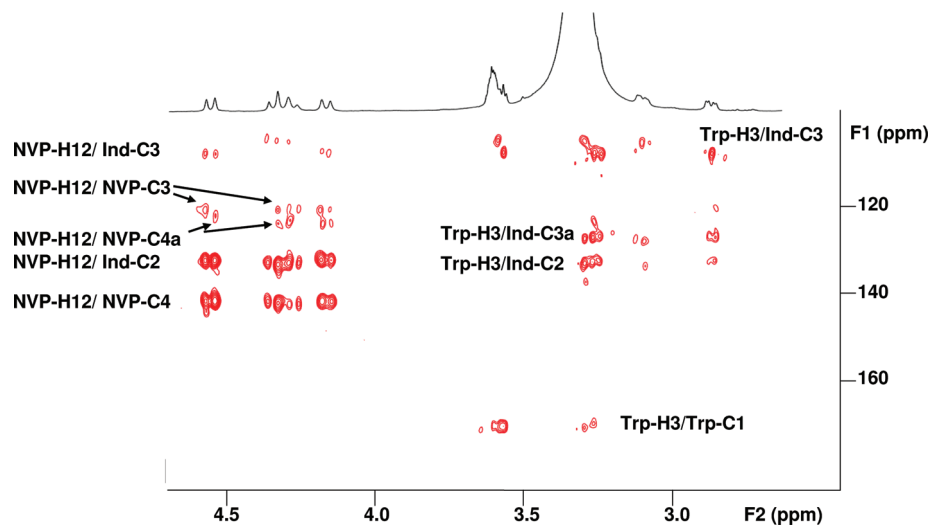
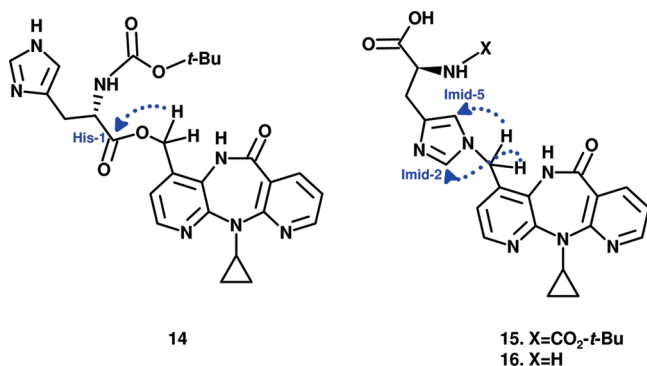


Figure 3. Expanded region of the ^1H - ^{13}C semiselective HMBC spectrum of **13**, displaying the connectivities between the geminal NVP-H12 protons and the carbons of the NVP (C3, C4, and C4a) and tryptophan (Ind-C2 and Ind-C3) moieties. The connectivities to the C2 and C3 carbons of the Ind ring of tryptophan were decisive in ascribing the Ind C2 as the binding site in tryptophan. Also shown are connectivities between the H3 protons in the aliphatic chain of tryptophan (Trp-H3) and the carbons of the amino acid, both in the aliphatic chain (the carboxylate, Trp-C1) and the Ind ring (Ind-C2, Ind-C3 and Ind-C3a).

Scheme 7. Structures of 14–16, Obtained in the Reaction of 9 with N^α -Boc-histidine (14 and 15) and Histidine (16)^a



^a The arrows represent the HMBC correlations of the NVP-H12 protons with specific carbons of the amino acid moieties.

resulting spectrum (Figure 3), recorded with spectral windows from 5.0 to 2.0 ppm (^1H) and from 100.0 to 180.0 ppm (^{13}C), showed the expected two- and three-bond correlations between the NVP H12 protons from both rotamers and carbons (C3, C4, and C4a) from the NVP moiety. In addition, correlations with two quaternary carbons of the tryptophan moiety, the Ind-C2 (at 133.3 and 133.8 ppm) and the Ind-C3 (at 108.2 and 109.1 ppm), were also observed. Taken together, these data are entirely consistent with connectivity between the NVP and tryptophan units through NVP-C12/Ind-C2. This regioselectivity was not unexpected since Inds are well-known to undergo electrophilic substitution at C2 whenever substitution blocks the reaction at the more electron-rich C3 position (35).

Reaction of **9** with N^α -Boc-histidine gave rise to a complex HPLC profile, due to the formation of multiple products. On the basis of LC/ESI-MS analysis (not shown) of four fractions separated by semipreparative HPLC, at least four adducts (m/z 520 for the protonated molecule) were present in the reaction mixture; nonetheless, only two of these adducts could be purified in quantities amenable to full spectral characterization. The two adducts, formed in 6 and 13% yields, were identified as **14** and **15**, respectively (Scheme 7). These species had almost identical LC/ESI-MS spectra, displaying both the protonated (m/z 520) and the diprotonated (m/z 261) molecules (not shown). Likewise,

the two adducts presented very similar ^1H NMR and ^{13}C NMR profiles, with all of the expected nonexchangeable resonances from the NVP and N -Boc-histidine moieties. The corresponding structures were discriminated on the basis of HMBC correlations between the NVP H12 protons and specific histidine carbons (Scheme 7). Thus, a three-bond correlation with the most downfield histidine carbon (the carboxylate, Hist-C1, at 172.3 ppm) was observed in adduct **14**, whereas adduct **15** displayed two three-bond correlations with carbons in the Imid ring of the histidine unit (Imid-C2, at 137.9 ppm, and Imid-C5, at 118.1 ppm). Moreover, the ^{13}C NMR spectrum of adduct **14** (Table 1) indicated a downfield shift of approximately 16 ppm for the NVP C12 resonance (detected at 62.0 ppm), as compared to that of adduct **15** (detected at 45.7 ppm), which is consistent with binding of the NVP C12 to an oxygen atom in adduct **14** (27). This observation further substantiates a direct connectivity between the NVP C12 and one of the oxygens from the histidine carboxylate in adduct **14**.

Considering that adduct formation through the histidine carboxylate will have negligible biological significance, with the possible exception of proteins with a C-terminal histidine, and bearing in mind that the typical pK_a of the Imid side chain is 6.5 (36), we investigated the direct reaction of **9** with free histidine. Because histidine is well-known to be sensitive to the microenvironment of the ionizable groups (37), we reasoned that, under our experimental conditions (pH 7.4), a zwitterionic form involving a protonated (and therefore non-nucleophilic) α -amino group would predominate, while a substantial fraction of the Imid side chain would remain unionized and thus available for nucleophilic attack. By using the nonprotected amino acid, we aimed to test whether predominant protonation on the α -amino group led to increased adduct formation through the Imid side chain. However, the reaction mixture was again rather complex, and several putative adducts, having very close retention times under a variety of elution conditions, were detected. This complexity presumably results from a combination of factors, including different protonation sites and tautomerism, which confer nucleophilic properties to all available positions (i.e., the two nitrogens and the two nonsubstituted carbons) of the Imid ring. Because of the complexity of the reaction mixture, we could only characterize one adduct, **16**

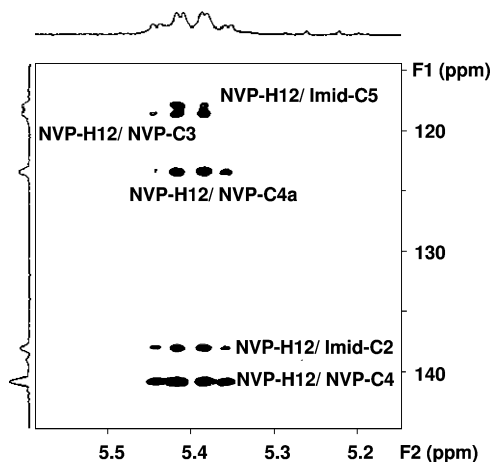
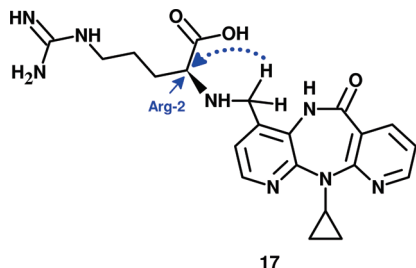


Figure 4. Expanded region of the ^1H - ^{13}C semiselective HMBC spectrum of **16**, displaying the connectivities between the geminal NVP-H12 protons and the carbons of the NVP (C3, C4, and C4a) and histidine (Imid-C2 and Imid-C5) moieties. The connectivities to the C2 and C5 carbons of the Imid ring of histidine were decisive in ascribing the Imid N1 as the binding site in histidine.

Scheme 8. Structure of 17, Obtained in the Reaction of 9 with Arginine^a

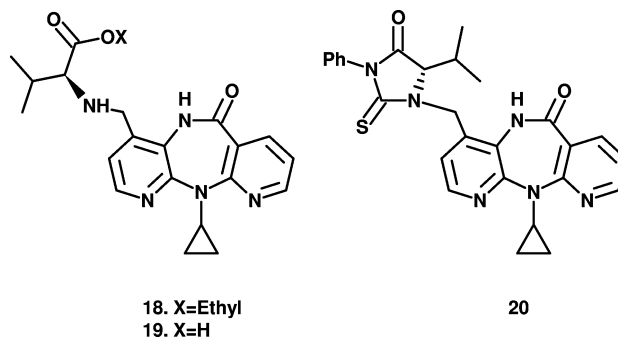


^a The arrow represents the HMBC correlation of the NVP-H12 protons with the arginine C2, which was decisive to assign the binding site.

(Scheme 7), which was isolated in 10% yield. The LC/ESI-MS spectrum of **16** showed both the protonated (m/z 420) and the diprotonated (m/z 211) molecules, and the ^1H NMR spectrum indicated the presence of all of the expected NVP protons, with the geminal H12 protons appearing as a multiplet centered at 5.41 ppm, suggestive of C12 binding to a heteroatom. Although it was not possible to obtain a ^{13}C NMR spectrum of **16** with a good signal/noise ratio, carbon resonance assignments were performed on the basis of the correlations observed in the more sensitive inverse bidimensional HMQC and HMBC experiments. Moreover, a semiselective HMBC experiment allowed the observation of three-bond correlations between the NVP-H12 protons and the Imid carbons at 119.9 (Imid-C5) and 138.0 (Imid-C2) ppm (Figure 4); these correlations were entirely consistent with a connectivity through NVP-C12/Hist-N1', which corroborated the structure assignment.

Reaction of **9** with arginine resulted in the formation of **17** (Scheme 8) in 6% yield. The first evidence for the formation of an arginine adduct was achieved by LC/ESI-MS analysis, which indicated the presence of the protonated (m/z 439) and diprotonated (m/z 220) molecules. Although displaying all of the expected nonexchangeable signals from the NVP and arginine moieties, both the ^1H NMR and the ^{13}C NMR spectra were again rather complex due to the existence of duplicate resonances (not shown). As observed for other adducts, in particular the tryptophan derivative **13**, the signal duplication suggests restricted rotational mobility between the amino acid and the NVP fragments, with two predominant conformers. Clear indication of the binding position between the two units was achieved by

Scheme 9. Structures of 18, Obtained in the Reaction of 9 with Ethyl Valinate, the Valine Adduct (19), and the Thiohydantoin Derivative (20)



analysis of the three-bond correlation profile observed in the HMBC spectrum (Scheme 8), where the arginine C2 of both rotamers (detected at 61.3 and 62.2 ppm) had connectivities to the NVP H12 protons (3.57–3.88 ppm), which is only possible with binding of the NVP C12 through the α -amino nitrogen of arginine. The lack of reaction at the terminal guanidino group presumably stems from the high basicity of this side chain group ($\text{p}K_a = 12.0$, ref 36), which suggests that arginine residues in proteins may be unlikely targets for electrophilic NVP metabolites.

The N-terminal valine residues in hemoglobin are primary sites of reaction with several classes of electrophiles. The binding products thus formed can be analyzed either as valine adducts, upon total hydrolysis of the protein, or as hydantoins (e.g., phenylthiohydantoins), upon an "N-alkyl Edman" procedure (38). Because hemoglobin is a suitable protein for biomonitoring studies, we also sought to obtain an NVP-valine adduct standard. The reaction of ethyl valinate with **9** resulted in the formation of **18** (Scheme 9) in 33% yield; subsequent basic hydrolysis of **18** gave **19** (Scheme 9) in 86% yield. LC/ESI-MS analysis showed the sodiated and protonated molecules (m/z 432 and 410, respectively) for **18** and the protonated molecule (m/z 382) for **19**. The ^1H and ^{13}C NMR spectra of both species displayed all of the expected resonances, although the spectra were rather complex, due to the existence of duplicate resonances, again suggesting restricted rotational mobility between the amino acid and the NVP fragments, with two predominant conformers. Nonetheless, the NVP-C12/Val-N^α connectivity was unequivocally ascribed on the basis of three-bond correlations in the HMBC spectra between the geminal NVP H12 protons of each conformer (e.g., two sets of doublets at 3.56/4.01 and 3.70/3.80 ppm in **19**) and the corresponding valine C2 (65.9 and 67.5 ppm, respectively).

The N-alkyl Edman procedure leads to the specific detachment of adducted valine residues as phenylthiohydantoins (38). This method was originally developed for GC-MS analysis, which explains the common use of a fluorinated phenyl isothiocyanate, but its application to polar, thermolabile, and high molecular weight adducts was limited. However, recent modifications, using LC-MS/MS for the measurement of valine adducts derivatized with phenyl isothiocyanate, have successfully broadened the scope of the method (39). Because of the anticipated low volatility of NVP-related phenylthiohydantoins, the LC-MS/MS methodology seems a suitable approach for the prospective analysis of these species, following *ex vivo* derivatization of NVP-modified hemoglobin. Thus, we also prepared a **20** (Scheme 9) standard by reaction of **18** with phenyl isothiocyanate. The LC-ESI-MS spectrum of the product exhibited the expected protonated molecule (m/z 499) and a characteristic fragment ion (m/z 265) stemming from loss of

the phenylthiohydantoin moiety. The ^1H NMR spectrum was entirely consistent with two stable conformers of **20**. Moreover, although we were unable to obtain a ^{13}C NMR spectrum of **20** with a good signal/noise ratio, carbon resonance assignments were performed on the basis of correlations observed in the more sensitive inverse bidimensional HMQC and HMBC experiments. For instance, three-bond correlations were detected in the HMBC spectrum between each specific set of geminal NVP-H12 protons and the thiohydantoin C5 (64.8 and 66.2 ppm) and thiocarbonyl C2 (183.4 ppm) of the corresponding conformer, which further confirmed the ascribed structure.

Conclusions

The role of metabolism in the toxic responses associated with NVP administration remains largely unknown, although recent evidence increasingly suggests the involvement of electrophilic metabolites, particularly through functionalization at C12, either via sulfation or generation of a quinone methide (21, 24–26). Our first report (27) on the use of **9** as a surrogate for **7** allowed us to synthesize and characterize a series of nucleoside and dephurinating NVP–DNA adducts which, if formed in vivo, could be relevant to NVP-induced hepatotoxicity. Despite the fact that the sulfate anion (SO_4^{2-}) is the conjugate base of a weak acid ($\text{p}K_a \sim 2$) whereas mesylate is the conjugate base of a strong acid ($\text{p}K_a \sim -2$) (40), a difference that may determine distinct reactivities and regioselectivities (i.e., C–O versus S–O bond cleavage) toward substitution and hydrolysis reactions (41), we were confident that our model is not unreasonable. In fact, aliphatic nucleophilic substitution reactions on monoalkylsulfates, involving sulfate displacement, have been described (42) and in some instances proceeded quite readily (43). Nonetheless, at the time of our study, even the formation of **7** in vivo was still speculative. However, the recent reports of the detection of **7** in vivo (21, 26), as well as of an NVP–GSH conjugate (25, 26) and an NVP–mercapturate (26), both inferred to involve binding through the NVP C12, have contributed decisively to reinforce our initial hypothesis. Although it may be argued that trapping of **7** (or its quinone methide derivative) by GSH can provide an efficient detoxification pathway, a similar reaction with nucleophilic side chains in proteins could be at the onset of toxic responses. To our knowledge, NVP–protein binding has yet to be addressed.

In the present manuscript, we have tested the reaction of the model electrophile **9** toward GSH, ethyl valinate, and a series of selected α -amino acids bearing nucleophilic side chains, with the aim of gaining insight into potentially reactive sites in proteins and obtaining well-characterized NVP–amino acid adduct standards. The resulting adducts consistently involved aralkylation of the amino acid residues through C12 of the NVP moiety. We obtained very efficient (>80%) binding through the sulfur of both GSH and *N*-acetylcysteine, significant binding (33%) through the α -amino group of valine, and moderate yields (10–14%) for binding through C2 of the Ind ring of tryptophan and N1 of the Imid ring of histidine. Reaction with arginine proceeded via binding through the α -amino group, presumably due to the high basicity of the guanidino group in the side chain. Regardless of the amino acid, there was consistent evidence of conformational heterogeneity in the synthetic adducts, presumably due to intramolecular hydrogen bonding; whether or not this heterogeneity will subsist in NVP-modified proteins remains to be established. The structures of the sulfur conjugates (**10** and **11**), which are identical to those reported to be formed in vivo (21, 25, 26), are fully characterized herein for the first time, by a combination of ^1H and ^{13}C NMR spectroscopy and mass

spectrometry techniques. Moreover, the ready formation of tryptophan–NVP and histidine–NVP adducts suggests that, besides the sulfur atoms in cysteine residues, the heteroaromatic side chains of these amino acids are plausible targets for protein modification by **5**-derived electrophiles in vivo. Likewise, the N-terminal valine residue in hemoglobin is a good candidate as a marker of NVP–protein binding in vivo. In conclusion, our results support the validity of the model electrophile **9** as a surrogate for the NVP metabolite, **7**, which may be used to provide reliable, fully characterized standards for the assessment of protein modification by NVP in vivo. This approach should help clarify the potential role of metabolism in NVP-induced toxicity. We are currently using the adduct standards reported herein for a comprehensive study of binding of **9** to model proteins in vitro using MS-based methodology. The optimized analytical procedures will then be applied to assess potential correlations between NVP administration and toxic responses in vivo.

Acknowledgment. We thank Thomas Heinze and Conceição Oliveira for the MS analyses. Thanks are also due to the Portuguese NMR Network (IST-UTL Center) and the Portuguese MS Network (IST-UTL Center) for providing access to the facilities. This work was supported in part by a research grant from Fundação para a Ciência e a Tecnologia (FCT), Portugal, and FEDER (POCI/QUI/56582/2004; PPCDT/QUI/56582/2004), by a postdoctoral fellowship (BPD/SFRH/27563/2006) from FCT to G.C.J., and by Interagency Agreement No. 224-93-0001 between the National Center for Toxicological Research/Food and Drug Administration and the National Institute for Environmental Health Sciences/National Toxicology Program. The opinions expressed in this paper do not necessarily represent those of the U.S. Food and Drug Administration.

Supporting Information Available: ^1H NMR spectra of **10** (Figure S1) and **11** (Figure S2), recorded in $\text{DMSO}-d_6$. This material is available free of charge via the Internet at <http://pubs.acs.org>.

References

- (1) FDA (1996) FDA approves nevirapine to treat HIV. News release T96-44, June 24, 1996.
- (2) Marseille, E., Kahn, J. G., Mmiro, F., Guay, L., Musoke, P., Fowler, M. G., and Jackson, J. B. (1999) Cost effectiveness of single-dose nevirapine regimen for mothers and babies to decrease vertical HIV-1 transmission in sub-Saharan Africa. *Lancet* 354, 803–809.
- (3) Jackson, J. B., Musoke, P., Fleming, T., Guay, L. A., Bagenda, D., Allen, M., Nakabiito, C., Sherman, J., Bakaki, P., Owor, M., Ducar, C., Deseyve, M., Mwatha, A., Emel, L., Duefield, C., Mirochnick, M., Fowler, M. G., Mofenson, L., Miotti, P., Gigliotti, M., Bray, D., and Mmiro, F. (2003) Intrapartum and neonatal single-dose nevirapine compared with zidovudine for prevention of mother-to-child transmission of HIV-1 in Kampala, Uganda: 18-month follow-up of the HIVNET 012 randomised trial. *Lancet* 362, 859–868.
- (4) Lallemand, M., Jourdain, G., Le Coeur, S., Mary, J. Y., Ngo-Giang-Huong, N., Koetsawang, S., Kanchana, S., McIntosh, K., and Thaineua, V., for the Perinatal HIV Prevention Trial (Thailand) Investigators (2004) Single-dose perinatal nevirapine plus standard zidovudine to prevent mother-to-child transmission of HIV-1 in Thailand. *N. Engl. J. Med.* 351, 217–228.
- (5) Lockman, S., Shapiro, R. L., Smeaton, L. M., Wester, C., Thior, I., Stevens, L., Chand, F., Makhema, J., Moffat, C., Asmelash, A., Ndase, P., Arimi, P., van Widenfelt, E., Mazhani, L., Novitsky, V., Lagakos, S., and Essex, M. (2007) Response to antiretroviral therapy after a single, peripartum dose of nevirapine. *N. Engl. J. Med.* 356, 135–147.
- (6) Pollard, R. B., Robinson, P., and Dransfield, K. (1998) Safety profile of nevirapine, a nonnucleoside reverse transcriptase inhibitor for the treatment of human immunodeficiency virus infection. *Clin. Ther.* 20, 1071–1092.

- (7) Mirochnick, M., Clarke, D. F., and Dorenbaum, A. (2000) Nevirapine: pharmacokinetic considerations in children and pregnant women. *Clin. Pharmacokinet.* 39, 281–293.
- (8) Waters, L., John, L., and Nelson, M. (2007) Non-nucleoside reverse transcriptase inhibitors: a review. *Int. J. Clin. Pract.* 61, 105–118.
- (9) Six Week Extended-Dose Nevirapine (SWEN) Study Team (2008) Extended-dose nevirapine to 6 weeks of age for infants to prevent HIV transmission via breastfeeding in Ethiopia, India, and Uganda: an analysis of three randomised controlled trials. *Lancet* 372, 300–313.
- (10) Phadke, M. A., Bulakh, P. M., and Kshirsagar, N. A. (2008) Nevirapine to prevent HIV transmission via breastfeeding. *Lancet* 372, 287.
- (11) Anonymous (2009) *Physicians' Desk Reference*, 63rd ed, pp 873–881, Physicians' Desk Reference Inc., Montvale, NJ.
- (12) Powles, T., Robinson, D., Stebbing, J., Shamash, J., Nelson, M., Gazzard, B., Mandelia, S., Möller, H., and Bower, M. (2009) Highly active antiretroviral therapy and the incidence of non-AIDS-defining cancers in people with HIV infection. *J. Clin. Oncol.* 27, 884–890.
- (13) Takakusa, H., Masumoto, H., Yukinaga, H., Makino, C., Nakayama, S., Okazaki, O., and Sudo, K. (2008) Covalent binding and tissue distribution/retention assessment of drugs associated with idiosyncratic drug toxicity. *Drug Metab. Dispos.* 36, 1770–1779.
- (14) Riska, P., Lamson, M., MacGregor, T., Sabo, J., Hattox, S., Pav, J., and Keirns, J. (1999) Disposition and biotransformation of the antiretroviral drug nevirapine in humans. *Drug Metab. Dispos.* 27, 895–901.
- (15) Riska, P. S., Joseph, D. P., Dinallo, R. M., Davidson, W. C., Keirns, J. J., and Hattox, S. E. (1999) Biotransformation of nevirapine, a non-nucleoside HIV-1 reverse transcriptase inhibitor, in mice, rats, rabbits, dogs, monkeys, and chimpanzees. *Drug Metab. Dispos.* 27, 1434–1447.
- (16) Erickson, D. A., Mather, G., Trager, W. F., Levy, R. H., and Keirns, J. J. (1999) Characterization of the in vitro biotransformation of the HIV-1 reverse transcriptase inhibitor nevirapine by human hepatic cytochromes P-450. *Drug Metab. Dispos.* 27, 1488–1495.
- (17) Liu, Z., Fan-Havard, P., Xie, Z., Ren, C., and Chan, K. K. (2007) A liquid chromatography/atmospheric pressure ionization tandem mass spectrometry quantitation method for nevirapine and its two oxidative metabolites, 2-hydroxynevirapine and nevirapine 4-carboxylic acid, and pharmacokinetics in baboons. *Rapid Commun. Mass Spectrom.* 21, 2734–2742.
- (18) Ren, C., Fan-Havard, P., Schlabritz-Loutsevitch, N., Ling, Y., Chan, K. K., and Liu, Z. (2010) A sensitive and specific liquid chromatography/tandem mass spectrometry method for quantification of nevirapine and its five metabolites and their pharmacokinetics in baboons. *Biomed. Chromatogr.* DOI: 10.1002/bmc.1353.
- (19) Silverman, R. B. (2004) *The Organic Chemistry of Drug Design and Drug Action*, 2nd ed., pp 1–617, Elsevier Academic Press, London, United Kingdom.
- (20) Bolton, J. L., Trush, M. A., Penning, T. M., Dryhurst, G., and Monks, T. J. (2000) Role of quinones in toxicology. *Chem. Res. Toxicol.* 13, 135–160.
- (21) Chen, J., Mannargudi, B. M., Xu, L., and Uetrecht, J. (2008) Demonstration of the metabolic pathway responsible for nevirapine-induced skin rash. *Chem. Res. Toxicol.* 21, 1862–1870.
- (22) Shenton, J. M., Teranishi, M., Abu-Asab, M. S., Yager, J. A., and Uetrecht, J. P. (2003) Characterization of a potential animal model of an idiosyncratic drug reaction: nevirapine-induced skin rash in the rat. *Chem. Res. Toxicol.* 16, 1078–1089.
- (23) Shenton, J. M., Popovic, M., Chen, J., Masson, M. J., and Uetrecht, J. P. (2005) Evidence of an immune-mediated mechanism for an idiosyncratic nevirapine-induced reaction in the female Brown Norway rat. *Chem. Res. Toxicol.* 18, 1799–1813.
- (24) Popovic, M., Caswell, J. L., Mannargudi, B., Shenton, J. M., and Uetrecht, J. P. (2006) Study of the sequence of events involved in nevirapine-induced skin rash in Brown Norway rats. *Chem. Res. Toxicol.* 19, 1205–1214.
- (25) Wen, B., Chen, Y., and Fitch, W. L. (2009) Metabolic activation of nevirapine in human liver microsomes: dehydrogenation and inactivation of cytochrome P450 3A4. *Drug Metab. Dispos.* 37, 1557–1562.
- (26) Srivastava, A., Lian, L.-Y., Maggs, J. L., Chaponda, M., Pirmohamed, M., Williams, D. P., and Park, B. K. (2010) Quantifying the metabolic activation of nevirapine in patients by integrated applications of NMR and mass spectrometries. *Drug Metab. Dispos.* 38, 122–132.
- (27) Antunes, A. M. M., Duarte, M. P., Santos, P. P., Gamboa da Costa, G., Heinze, T. M., Beland, F. A., and Marques, M. M. (2008) Synthesis and characterization of DNA adducts from the HIV reverse transcriptase inhibitor nevirapine. *Chem. Res. Toxicol.* 21, 1443–1456.
- (28) Marques, M. M., Martins, I., Antunes, A. M. M., Santos, P. P., Gamboa da Costa, G., and Beland, F. A. (2008) Synthesis and characterization of amino acid adducts from the HIV reverse transcriptase inhibitor nevirapine. *Chem. Res. Toxicol.* 21, 2453; Abstract 105.
- (29) Perrin, D. D., and Armarego, W. L. F. (1988) *Purification of Laboratory Chemicals*, 3rd ed., pp 1–391, Pergamon Press, Oxford, United Kingdom.
- (30) Mayo, S. L., Olafson, B. D., and Goddard, W. A., III (1990) DREIDING: a generic force field for molecular simulations. *J. Phys. Chem.* 94, 8897–8909.
- (31) ChemAxon (2008) Marvin version 5.00 and Calculator Plugins for Marvin version 5.00, ChemAxon, Budapest, Hungary (<http://www.chemaxon.com>).
- (32) Stewart, J. J. P. (2007) Optimization of parameters for semiempirical methods V: modification of NDDO approximations and application to 70 elements. *J. Mol. Model.* 13, 1173–1213.
- (33) Stewart, J. J. P. (2008) MOPAC2009, Stewart Computational Chemistry, Colorado Springs, CO (<http://OpenMOPAC.net>).
- (34) Rezáč, J., Fanfrlík, J., Salahub, D., and Hobza, P. (2009) Semiempirical quantum chemical PM6 method augmented by dispersion and H-bonding correction terms reliably describes various types of noncovalent complexes. *J. Chem. Theory Comput.* 5, 1749–1760.
- (35) Brown, R. T., and Joule, J. A. (1979) In *Heterocyclic Chemistry* (Sammes, P. G., Ed.) Vol. 4 of Comprehensive Organic Chemistry (Barton, D., and Ollis, W. D., Eds.) p 411, Pergamon Press, Oxford, United Kingdom.
- (36) Berg, J. M., Tymoczko, J. L., and Stryer, L. (2006) *Biochemistry*, 6th ed., 1050 pp, W.H. Freeman & Co., New York.
- (37) Miyagi, M., and Nakazawa, T. (2008) Determination of pK_a values of individual histidine residues in proteins using mass spectrometry. *Anal. Chem.* 80, 6481–6487.
- (38) Törnqvist, M., Fred, C., Haglund, J., Helleberg, H., Paulsson, B., and Rydberg, P. (2002) Protein adducts: quantitative and qualitative aspects of their formation, analysis and applications. *J. Chromatogr. B* 778, 279–308.
- (39) Chevolleau, S., Jacques, C., Canlet, C., Tulliez, J., and Debrauwer, L. (2007) Analysis of hemoglobin adducts of acrylamide and glycidamide by liquid chromatography-electrospray ionization tandem mass spectrometry, as exposure biomarkers in French population. *J. Chromatogr. A* 1167, 125–134.
- (40) Smith, M. B., and March, J. (2001) *March's Advanced Organic Chemistry. Reactions, Mechanisms, and Structure*, 5th ed., 2083 pp, Wiley Interscience, New York.
- (41) Wallner, S. R., Nestl, B., and Faber, K. (2005) Stereoselective hydrolysis of *sec*-mono-alkyl sulfate esters with retention of configuration. *Tetrahedron* 61, 1517–1521.
- (42) Fraser, A. S., Kawasaki, A. M., Jung, M. E., and Manoharan, M. (2000) An efficient method for the synthesis of 2'-O-modified nucleosides via double alkylation using cyclic sulfates. *Tetrahedron Lett.* 41, 1523–1526.
- (43) Watabe, T., Hakamata, Y., Hiratsuka, A., and Ogura, K. (1986) A 7-hydroxymethyl sulphate ester as an active metabolite of the carcinogen, 7-hydroxymethylbenz[a]anthracene. *Carcinogenesis* 7, 207–214.

TX900443Z